BEHAVIOUR OF A FRP ANCHOR FOR SEISMIC STRENGTHENING OF CLAY BRICK MASONRY WALLS

Yi Tao [1], Ling-Jun Zhong [1], Jiaping Liu [2] and Jian-Fei Chen[3,*]
[1] School of Civil Engineering, Xian University of Architecture and Technology, Xian, China.
[2] School of Architecture, Xian University of Architecture and Technology, Xian, China.
[3] School of Planning, Architecture, and Civil Engineering, Queen's Univ. Belfast,
Belfast, BT9 5AG, U.K. *Email:j.chen@qub.ac.uk

ABSTRACT

Fibre reinforced polymer (FRP) anchors made from rolled or folded fibres have been shown to be an effective technology for delaying or even preventing premature debonding failure in concrete structures strengthened with externally bonded FRP. It would naturally be expected that the use of FRP anchors can improve the earthquake-resistance of FRP strengthened structures by increasing its loading capacity and ductility especially the latter. This study explores the application of FRP anchors in seismic strengthening of clay brick walls. One unique feature of such a system is that the brick unit has smaller dimensions compared to common concrete specimens. This paper reports an experimental pull out study of these FRP anchors. Test parameters included anchor construction, the diameter of the anchor, and the size of predrilled holes in clay brick. The experimental results indicate that FRP anchors can be designed to achieve high loading capacities and hence can be effectively used to prevent or delay FRP debonding failure. The results also indicate that the geometry of the anchor system has a significant effect on its loading capacity.

KEYWORDS

FRP anchor, masonry, anchorage strength, experiment.

INTRODUCTION

There has being an explosive increasing demand for retrofitting existing structures to improve their performance, especially to enhance their earthquake-resistance. The use of FRP strengthening system has recently emerged as one of the advanced retrofitting techniques. Although this technique has been proved to be a convenient and effective approach, existing studies have also demonstrated that externally bonded FRP tends to exhibit premature debonding from the substrate, prior to the development of full material strength (Smith, et al., 2011), leading to reduced seismic performance of FRP strengthened structures due to the brittleness and low energy dissipation capacity.

One effective and rational approach for preventing or delaying debonding is the use of proper anchor technologies, commonly including metal anchors to mechanically fasten the FRP sheet to substrate and FRP anchor to be embedded into a predrilled hole in substrate using epoxy (Ozbakkaloglu and Saatcioglu, 2009, Smith, et al., 2011, Zhang, et al., 2012). The former often results in bearing failure of the FRP due to stress concentrations around the anchor. FRP anchors can usually avoid or minimise this problem because the fibres from the anchor are spread out and bonded to the FRP sheet. It has an added advantage of being the same corrosion-resistant material of the strengthening FRP. A FRP anchor consists of a rolled or folded FRP strip embedded into a predrilled hole in substrate using adhesive. Existing research has demonstrated that the utilization of FRP anchors can effectively improve the seismic performance in terms of loading carry capacity and energy dissipation capability.

The vast majority of existing studies of FRP anchors has been concerned with concrete structures. Little research has been conducted on the pullout behaviour of FRP anchors installed into masonry, especially clay brick masonry. One feature of such a system is that brick units have smaller dimensions compared to common concrete specimens.

This paper reports an experimental study on the pullout behaviour of FRP anchors embedded into clay bricks. The effects of important parameters, including brick strength, hole diameter, anchor embedment (hole) depth, and anchor fiber content on the pullout behaviour were examined. An anchorage strength model is proposed which may be adopted for design use. This study forms part of a project on seismic strengthening of masonry structures using a hybrid FRP grid-FRP anchor system.

EXPERIMENTAL STUDY

A total of 42 CFRP anchors were manufactured and tested under pullout action. The test parameters included the anchor construction, embedment depth, hole diameter, fibre content and brick strength.

FRP anchor construction

FRP anchors can be formed either dry or wet and both were explored in this study: the former uses dry FRP strips to form a bar for the embedded portion whilst the latter uses wet FRP strips. FRP anchors are then constructed commonly by rolling the pre-cut FRP sheet, either dry or wetted. However, the rolling usually leads to fibre congestion at the centre of the anchor leading to difficulties in wetting the fibres in the centre in the dry process. An alternative method is to prepare the anchor by folding the sheet in order to have more uniform wetting of the fibres.

To investigate the performance of the different FRP anchor construction methods, three types of FRP anchors were explored in the present study: anchors made by rolling dry FRP strips, folding dry FRP strips, and folding wet FRP strips. For both rolling and folding dry FRP anchors, a FRP strip with the desired size was cut from a large FRP sheet, which was then rolled or folded to form an anchor. For impregnated (wet) FRP anchor, a thin layer of epoxy was used to wet the area of the FRP strip which would be embedded into bricks after folding.

The material properties of the CFRP and epoxy resin used to manufacture the FRP anchors are summarized in Table 1. The two critical parameters in determining the width of FRP strip were: (1) the tensile capacity of FRP anchors, and (2) the content of FRP and epoxy inside the predrilled hole. As the interested failure mode was the pullout failure of FRP anchors, the anchors were thus designed to have sufficient amount of fibres to prevent the rupture anchor failure in pullout test.

Table 1 Properties of CFRP sheet and epoxy used in manufacturing FRP anchors (from manufacturer)

Material	Nominal thickness (mm/ply)	Ultimate tensile strength (MPa)	Elastic modulus (MPa)	Rupture strain (%)
CFRP sheet	0.167	3400	230000	1.7
Epoxy resin	-	30	4500	0.9

Brick specimens

Two types of solid clay bricks were used in this study: one had compressive strength and bending tensile strength of 21.7 MPa and 3.16 MPa respectively and the other had compressive strength and bending tensile strength of 31.1 MPa and 5.35 MPa respectively. All the bricks had nominal dimensions of 240×115×53 mm^3. The strengths were tested following the Chinese standard GB 5101-2003 (2003).

Anchor installation

A rotary hammer drill was used to drill the holes to a depth equal to the designed embedment length of anchors in the clay bricks. The holes were cleaned using compressed air. They were then filled with a two component epoxy adhesive using a syringe. Two 0.9mm diameter steel wires were bound together and used to stir the adhesive in order to make it uniform and consistent and eliminate air pockets. The anchors were then inserted into the holes perpendicular to the brick face. The free end of FRP anchors were adhesively clamped using two aluminium plates after 2 days of installing the FRP anchors. All specimens were cured at room temperature for 3 days prior to testing.

Test setup

All specimens were tested using a 300 kN universal testing machine. The test set up is shown in Figure 1. The pullout tests were conducted under displacement control at a loading rate of 2 mm/min. In addition to the load, the displacement of FRP and bricks were monitored using both LVDTs and the PIV technique (Figure 1 (b)).

TEST RESULTS AND DISCUSSION

The pullout behaviour of FRP anchors were analysed as follows. Table 2 summarises the key test parameters and results.

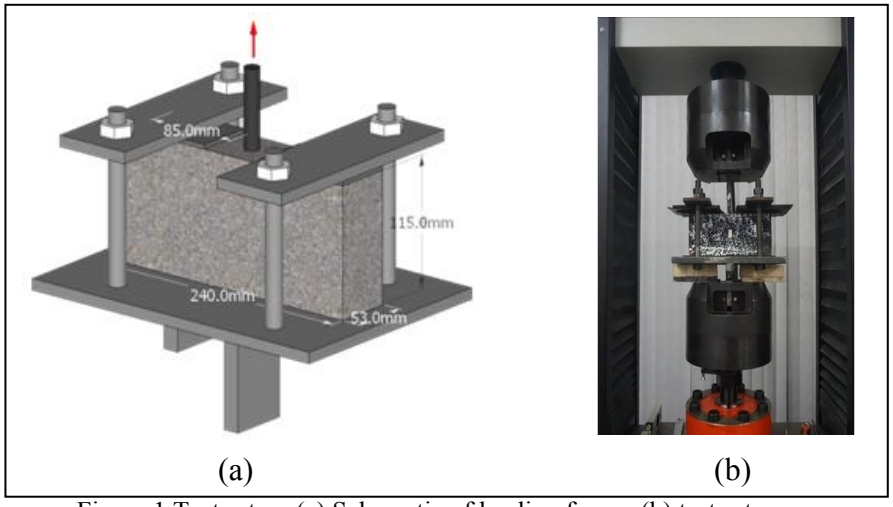

Figure 1 Test setup: (a) Schematic of loading frame, (b) test setup

Failure modes

The failure modes may be classified into four types: Type A - mixed mode with a triangular prism detached from and a unsymmetrical splitting crack into the brick [Figure 2 (a)], Type B - a triangular prism detached from the brick [Figure 2 (b)], Type C– mixed mode with a triangular prism detached from and a symmetrical splitting crack into the brick [Figure 2 (c)], and Type D – mixed mode with a triangular prism detached from the brick with a splitting crack along the embedded FRP anchor within the detached prism [Figure 2 (d)]. All failures are brittle. A brick triangular prism or similar shape is evident in all modes. Compared to the failure modes of FRP anchors embedded in concrete substrate, an important distinction is that a triangular prism is detached from the tested clay bricks whilst a cone occurs in concrete (Figure 3). This may be attributed to the smaller dimensions of the adopted bricks compared with the common concrete specimens. Existing analytical models developed for concrete cone failures may therefore not be applicable to brick anchorage failures because the projected area of the failure prism is rectangle in the bricks instead of a circular area in concrete specimens.

Optimization of FRP anchors

Three types of FRP anchors were used in this study, namely, rolling dry FRP strip (J type in Table 2), folding dry FRP strip (Z type in Table 2), and folding wet FRP strip (ZJX type in Table 2). Figure 4 illustrates the effect of anchor type on the average ultimate pullout load. It is shown that the folding wet FRP anchors provided the highest ultimate pullout load among the three types of anchors, because this anchor has good bond between the anchor and the brick as well as between fibres. The pullout behaviour of this anchor was thus investigated further.

Influence of key variables of FRP anchor

This section analyses the effects of key parameters of the ZJX type FRP anchors on the anchorage strength. The pullout strength versus anchor hole diameter is shown in Figure 5. It is seen that the ultimate pullout loads are very similar for hole diameter =10 and 12mm. Note that the average equivalent diameter of the folding wet FRP anchors was 9.1 mm, which means that there was only a very small amount of adhesive around the anchor in the holes and little working space when the hole diameter is small. When the hole diameter was increased to 14 mm, the ultimate pullout load was significantly improved, probably because improved bond between the anchor and masonry due to increased working space and bond area. Eight out of the nine specimens failed in modes exhibiting splitting cracks (Figures 2a, c, d) when the hole diameter was increased to 14 mm, only specimen ZJX-10 failed with a single brick chunk broken off (Figure 2b).

The pullout strength versus the anchor hole depth (anchorage length) is shown in Figure 6. It is clear that the deeper the hole the greater the ultimate pullout strength for a given hole diameter. The specimens with smaller hole depths (~20 mm) usually failed in modes without splitting cracks extending to the full height of brick (Figures 2b and d).

Table 2 Key parameters and test results of specimens

Specimen [+]	Geometry (mm)	Hole depth L_h (mm)	Hole diameter d_0(mm)	FRP anchor length (mm)	Embedment length (mm)	FRP width w (mm)	Equivalent diameter of FRP anchor[#](mm)	Test pullout load (kN)		Failure mode[##]
									Average [SD]*	
J-i-1	236×115×50	31.0	12.2	119.8	30.2	150	7.56	3.34	3.47 [0.25]	C
J-i-2	238×115×50	32.6	11.7	202.4	31.8		7.36	3.30		C
J-i-3	238×114×50	32.9	12.0	199.6	31.9		7.58	3.76		C
Z-i-1	236×113×49	30.2	11.8	205.3	29.7	150	7.56	5.22	5.14 [0.07]	B
Z-i-2	237×115×51	30.2	12.0	202.4	29.4		7.56	5.08		D
Z-i-3	236×117×50	29.9	12.3	202.5	28.7		7.52	5.13		D
ZJX-i-1	235×114×52	30.9	10.3	205.7	29.7	150	9.04	5.54	5.77 [0.31]	B
ZJX-i-2	237×113×48	29.7	10.1	199.5	28.4		8.87	6.11		B
ZJX-i-3	236×113×51	30.9	10.3	200.0	30.1		9.03	5.64		D
ZJX-i-4	239×116×50	31.8	11.6	200.1	30.6	150	8.54	5.42	5.65 [0.28]	C
ZJX-i-5	236×115×52	32.7	11.5	200.2	31.9		9.07	5.97		A
ZJX-i-6	237×114×50	32.7	11.5	200.2	31.9		9.07	5.57		A
ZJX-i-7	240×116×50	32.5	14.0	199.2	31.1	150	9.03	6.52	6.17 [0.32]	A
ZJX-i-8	236×114×50	30.7	14.1	200.0	30.0		9.55	6.10		D
ZJX-i-9	235×116×52	31.0	14.0	199.4	30.2		9.06	5.90		A
ZJX-i-10	239×115×51	20.1	10.1	200.1	21.0	150	9.01	3.86	3.84 [0.12]	D
ZJX-i-11	236×115×50	21.5	10.2	199.9	20.0		9.05	3.71		B
ZJX-i-12	238×114×52	22.1	10.0	201.1	19.8		8.94	3.95		D
ZJX-i-13	237×116×49	21.7	12.0	201.7	20.7	150	9.03	4.23	4.16 [0.21]	B
ZJX-i-14	239×115×51	20.4	12.0	201.0	19.8		8.72	3.93		B
ZJX-i-15	236×113×50	19.0	12.0	199.4	16.1		9.04	4.32		B
ZJX-i-16	235×114×49	22.3	14.0	215.5	21.8	150	8.89	4.90	4.98 [0.33]	A
ZJX-i-17	235×115×50	20.2	14.1	206.4	19.8		9.14	5.34		D
ZJX-i-18	237×115×52	20.4	14.1	205.8	18.9		9.09	4.70		B
ZJX-i-19	234×114×49	40.3	9.6	202.0	39.5	150	9.02	6.60	6.76 [0.54]	D
ZJX-i-20	236×114×52	41.2	10.1	200.0	40.0		8.98	7.36		A
ZJX-i-21	235×114×51	40.3	9.9	201.0	38.8		9.04	6.31		D
ZJX-i-22	240×116×53	39.9	12.4	200.8	38.4	150	9.01	6.24	6.15 [0.33]	D
ZJX-i-23	237×115×50	40.4	11.9	200.9	39.0		9.05	6.42		C
ZJX-i-24	238×114×50	43.4	12.2	201.7	42.2		9.11	5.78		C
ZJX-i-25	234×113×49	39.2	13.8	198.6	37.5	150	9.12	7.46	7.42 [0.21]	C
ZJX-i-26	236×116×50	39.7	14.0	203.1	38.7		8.97	7.61		A
ZJX-i-27	240×115×50	42.8	14.1	201.7	40.1		8.76	7.19		D
ZJX-i-28	240×116×53	30.3	12.0	200.7	30.1	50	5.10	4.89	4.73 [0.17]	B
ZJX-i-29	237×116×50	30.8	12.0	199.6	29.9		5.04	4.56		D
ZJX-i-30	239×116×51	31.5	12.2	200.5	30.0		5.08	4.75		D
ZJX-i-31	239×116×49	30.5	11.9	199.0	27.7	100	7.53	5.55	5.95 [0.38]	A
ZJX-i-32	239×115×51	33.8	12.1	199.5	32.5		7.24	5.99		A
ZJX-i-33	236×115×50	31.6	12.0	200.3	30.8		7.54	6.30		B
ZJX-ii-34	239×115×51	30.0	13.9	200.2	29.4	150	8.95	3.51	3.41 [0.15]	D
ZJX-ii-35	240×115×50	29.3	13.7	201.0	28.2		9.54	3.24		D
ZJX-ii-36	239×115×51	29.1	13.8	199.5	28.0		9.25	3.48		D

[+] J- rolling dry FRP strip, Z- folding dry FRP strip, ZJX- folding adhesive impregnated FRP strip, - i – high strength brick; - ii –low strength brick;

[#] equivalent diameter of FRP anchor was converted from the measured perimeter of finished anchor;

* [SD] – standard deviation;

[##] Failure Mode – corresponding to modes illustrated in Figure 2;

All notes are applied to all tables.

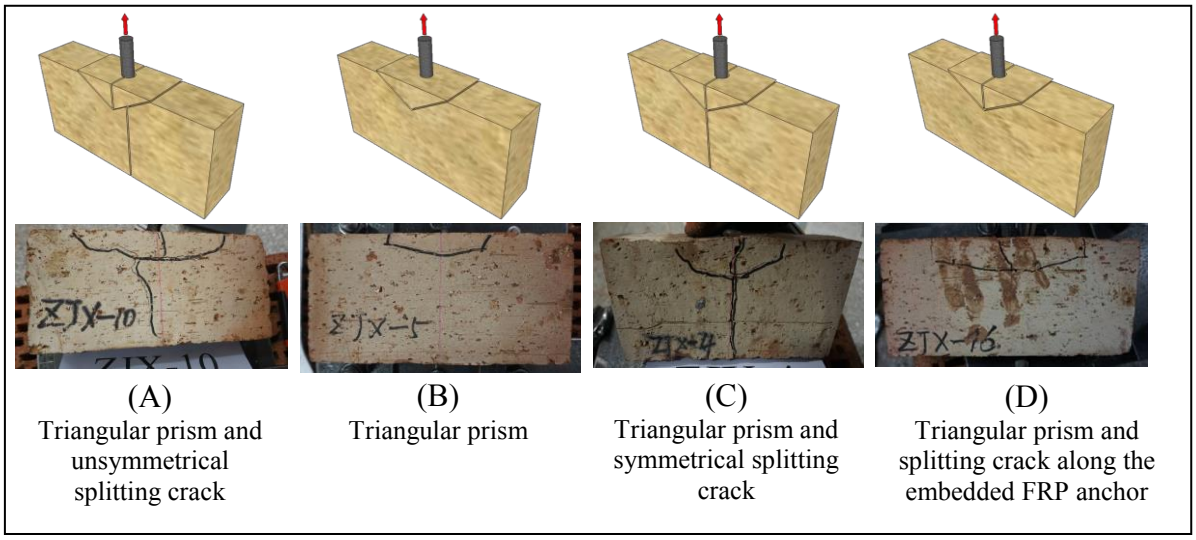

Figure 2. Failure modes

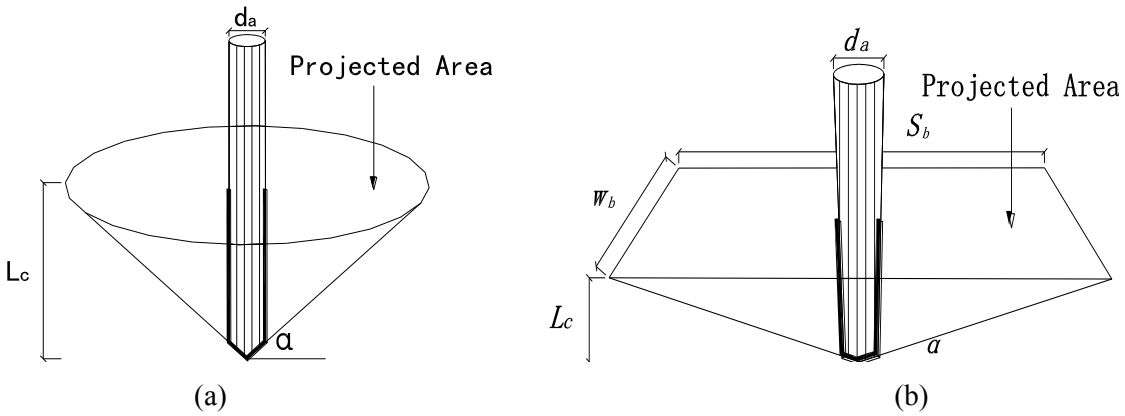

Figure 3 Different failure modes in concrete and clay brick

(a) concrete pullout cone, (b) clay brick pullout triangular prism

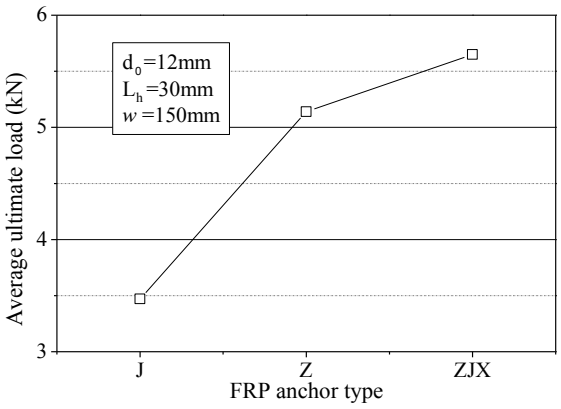

Figure 4. Effect of FRP anchor type on ultimate pullout load

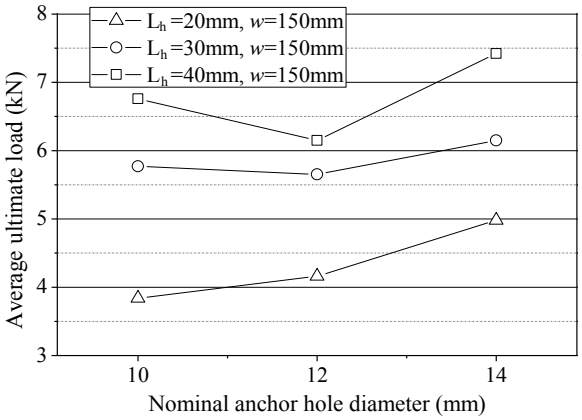

Figure 5. Effect of anchor hole size on ultimate pullout load (ZJX anchor)

The FRP strip width, also referred as equivalent anchor diameter converted from the perimeter of finish FRP anchors, versus the ultimate pullout load is plotted in Figure 7. It is interesting to note that the highest ultimate pullout load is experienced by anchors with a width of 100 mm (equivalent anchor diameter of 7.4 mm). The loading capacity was lower for specimens with 150mm FRP strips may be because less adhesive was used for the same hole diameter leading to weaker bond.

The lower brick strength led to a weaker pullout ultimate load as expected, e.g., the pullout strength from ZJX-ii-34 to 36 was lower than that from ZJX-i-7 to 9 as only brick strength were different in the two groups. All three low strength brick specimens (ZJX-ii-34 to 36) failed in the type D mode (Figure 2). That can be contributed to the pullout of FRP anchor due to cracks in the brick.

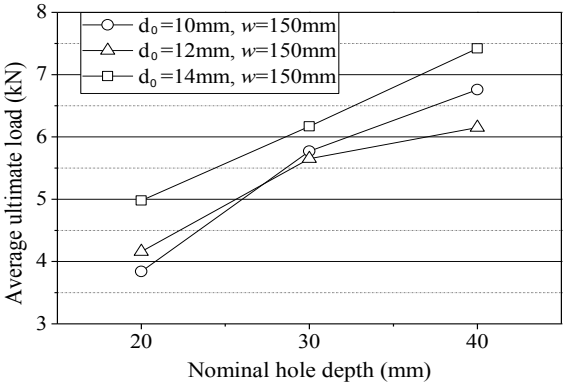

Figure 6. Effect of hole depth on ultimate pullout load (ZJX anchor)

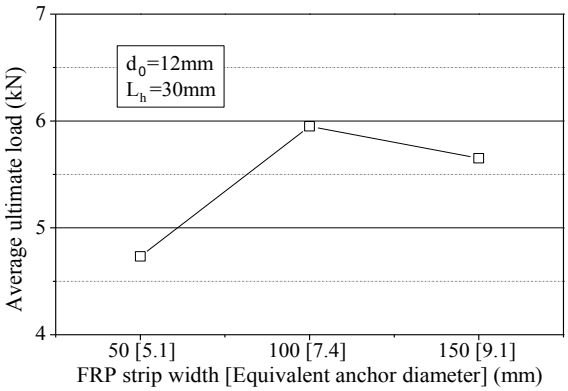

Figure 7. Effect of FRP strip width [equivalent anchor diameter] on ultimate pullout load (ZJX anchor)

PULLOUT STRENGTH MODEL FOR FRP ANCHORS IN CLAY BRICK

It was observed that a triangular prism was detached from the brick in all ZJX specimens. This failure pattern may thus be used as the base case for deriving the pullout capacity of FRP anchor in clay bricks. Compared with the cone failure of FRP anchor in concrete (Figure 3(a)), the triangular prism failure in clay bricks shared the similar failure manner but a different projected area due to the smaller dimensions of bricks. Assuming a cone angle (α) of 45 º based on a statistical analysis, Ozbakkaloglu and Saatcioglu (2009) proposed the following concrete cone capacity model based on the ACI 349-85 (1997) cone model:

$$F_{cone} = f_{ct} A_N = f_{ct} \cdot (\pi L_c^2 + \pi L_c d_a) \quad (1)$$

In which f_{ct} is the concrete tensile strength, A_N is the projected area of stress cone which consists of a circular area for the basal plane of the cone and the surface area of the bond, L_c is the depth of the concrete cone, and d_a is the diameter of the anchor as shown in Figure 3(a).

Equation 1 cannot be applied directly to the clay brick triangular prism failure for several reasons. Firstly, there is an apparent difference in the failure shapes. Secondly, the test results showed in this study that the pullout strength is influenced by not only the diameter of the anchor (d_a) but also that of the hole (d_0). Thirdly, it is found from the test that the triangular prism angle (α) (Figure 3b) varied with the anchor geometry. A new strength model is thus required for the triangular prism in bricks. By examining the failure prisms in detail, the projected failure area of the brick failure prism $(A_N)_{brick}$ (Figure 3(b)) may be expressed as

$$(A_N)_{brick} = w_b S_b + \pi L_c d_a = 2 \cdot w_b \cdot \frac{L_c}{\tan\alpha} + \pi L_c d_a \quad (2)$$

where w_b is the width of the brick, L_c is the depth of the triangular failure prism in the anchor direction, S_b is the length of the projected area, and α is the triangular angle.

Apart from the desired parameters w_b and d_a, the parameters related to the triangular prism failure pattern, such as, L_c and α, were measured in the experiment and recorded in Table 3. The depth of triangular prism (L_c) and the length of the projected area (S_b) were directly measured from the two sides of the brick as shown in Figure 8. It can found from Table 3 and Table 2 that the depth of triangular prism (L_c) was approximately equal to the hole depth (L_h). In order to develop a prediction model, the depth of triangular prism (L_c) in equation 2 is replaced by the hole depth (L_h) because it is a pre-defined parameter.

Table 3 Test and prediction results for ZJX type FRP anchors

Specimen	S_b	L_c	α (degree)		Pullout strength		
				Average [SD]	Test	Model (Eq. 5)	Test/Model
ZJX-i-1	82.3	29.5	35.6	27.8 [6.9]	5.54	4.73	1.17
ZJX-i-2	115.4	27.2	25.3		6.11		1.29
ZJX-i-3	141.1	29.3	22.5		5.64		1.19
ZJX-i-4	107.2	33.1	31.7	29.1 [3.4]	5.42	5.57	0.97
ZJX-i-5	116.3	27.5	25.3		5.97		1.07
ZJX-i-6	102.0	29.7	30.2		5.57		1.00
ZJX-i-7	134.3	30.3	24.3	22.7 [2.4]	6.52	6.41	1.02
ZJX-i-8	147.0	26.6	19.9		6.10		0.95
ZJX-i-9	131.2	29.1	23.9		5.90		0.92
ZJX-i-10	75.9	20.6	28.5	20.0 [7.6]	3.86	4.36	0.88
ZJX-i-11	142.4	17.8	14.0		3.71		0.85
ZJX-i-12	127.0	19.8	17.4		3.95		0.91
ZJX-i-13	135.1	17.5	14.6	19.3 [6.8]	4.23	5.17	0.82
ZJX-i-14	127.0	18.6	16.3		3.93		0.76
ZJX-i-15	67.6	17.3	27.1		4.32		0.84
ZJX-i-16	111.7	17.5	17.4	18.8 [1.2]	4.90	5.97	0.82
ZJX-i-17	128.1	22.8	19.6		5.34		0.89
ZJX-i-18	107.1	18.7	19.3		4.70		0.79
ZJX-i-19	135.2	39.7	30.4	30.8 [0.3]	6.60	5.10	1.29
ZJX-i-20	120.4	36.2	31.1		7.36		1.44
ZJX-i-21	121.7	36.3	30.8		6.31		1.24
ZJX-i-22	158.0	36.5	24.8	29.2 [3.8]	6.24	5.98	1.04
ZJX-i-23	108.5	33.8	31.9		6.42		1.07
ZJX-i-24	131.9	39.3	30.8		5.78		0.97
ZJX-i-25	124.3	38.0	31.5	28.5 [2.7]	7.46	6.86	1.09
ZJX-i-26	143.3	37.7	27.8		7.61		1.11
ZJX-i-27	179.1	44.3	26.3		7.19		1.05
ZJX-i-28	126.4	25.7	22.2	21.8 [1.9]	4.89	5.34	0.92
ZJX-i-29	147.4	26.6	19.8		4.56		0.85
ZJX-i-30	126.2	27.5	23.5		4.75		0.89
ZJX-i-31	139.0	31.1	24.1	25.7 [4.5]	5.55	5.47	1.01
ZJX-i-32	121.1	36.0	30.8		5.99		1.09
ZJX-i-33	139.5	28.6	22.3		6.30		1.15
ZJX-ii-34	123.9	25.8	22.6	21.7 [1.3]	3.51	3.79	0.93
ZJX-ii-35	132.1	27.0	22.2		3.24		0.85
ZJX-ii-36	136.6	25.1	20.2		3.48		0.92
						SD	0.16
						CoV	16%

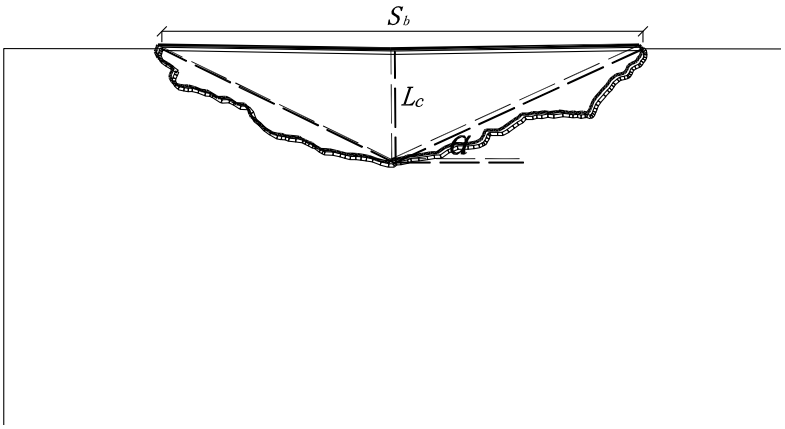

Figure 8. Brick triangular prism failure pattern

An approximation was adopted in calculating the triangular angle (α) in Table 3 by assuming that the triangular prism was symmetrical. A regression analysis of the test results shows that α can be closely related to the hole depth (L_h) and the hole diameter (d_0) as follows

$$\tan\alpha = 0.18\frac{L_h}{d_0} \tag{3}$$

The pullout strength model should consider all the critical parameters identified in the experiments, including hole depth (L_h), hole diameter (d_0) and diameter of anchor (d_a). The ratio of diameter of hole to the anchor (d_0/d_a) was chosen as an additional term to jointly consider the effects from both parameters. The pullout strength model was thud developed by a regression analysis as follows

$$(F)_{brick} = 0.115 \cdot f_{bt} \cdot \left\lfloor \frac{2hL_h}{\tan\alpha} + \pi L_h d_a \left(1 + \frac{d_0}{d_a}\right) \right\rfloor \tag{4}$$

where f_{bt} is the tensile strength of the brick.

Substituting equation (3) into equation (4) yields

$$(F)_{brick} = 0.115 \cdot f_{bt} \cdot \left\lfloor \frac{2hd_0}{0.18} + \pi L_c d_a \left(1 + \frac{d_0}{d_a}\right) \right\rfloor \tag{5}$$

It is clear that this new model is a prediction model because all parameters are pre-defined.

The statistical performance of the proposed model was examined by comparing its predictions with the test data as listed in Table 3. It is clear that the predictions of the proposed pullout strength model are in close agreement with the test data. However, the experimental data presented are limited, more test data are required to further validate the proposed model.

CONCLUSIONS

This paper has presented a study on the behaviour of FRP anchors embedded into clay bricks. Three types of FRP anchors were explored to optimize the FRP anchor manufacture approach. The influences of key parameters of the optimal FRP anchor, made by folding wet FRP strips, were investigated. It has been found that the geometry of the anchor system has a significant effect on the its loading capacity. An increase of the brick strength also increases the ultimate pullout strength. Finally, a new simple pullout strength model has been developed. This new model considers all the critical parameters based on the present test results and its prediction has been shown in close agreement with the test results.

ACKNOWLEDGMENTS

The authors acknowledge financial support received from National Basic Research Program (i.e. 973 Program) (2012CB026200) of China, the National Science Foundation of China (NSFC) (51408478), Science Foundation of ShaanXi Department of Education (14JK1437) and China Postdoctoral Science Foundation (2015M572529).

REFERENCES

American Concrete Institute (ACI) (1997). "Code requirements for nuclear safety related structures (ACI 349-85)". ACI Committee 394, Farmington Hills, Mich.

GB 5101-2003 (2003). "National Standard of China - Fired Common Brick". Beijing, China.

Ozbakkaloglu, T., and Saatcioglu, M. (2009). "Tensile Behavior of FRP Anchors in Concrete". Journal of Composites for Construction, 13(2), 82-92.

Smith, S. T., Hu, S., Kim, S. J., and Seracino, R. (2011). "FRP-strengthened RC slabs anchored with FRP anchors". Engineering Structures, 33(4), 1075-1087.

Zhang, H. W., Smith, S. T., and Kim, S. J. (2012). "Optimisation of carbon and glass FRP anchor design". Construction and Building Materials, 32, 1-12.